

## An elastic-Plastic Contact Model of a Sphere against a Hard Flat

**Jamari**

Mechanical Engineering Department, Faculty of Engineering, Diponegoro University  
Jl. Prof. Soedarto SH, Tembalang, Semarang 50275 Indonesia  
Telp/Fax: +62 24 7460059  
E-mail: j.jamari@gmail.com

### Abstract

*In this paper a theoretical model for the elastic-plastic microcontact model of asperities is presented. Relation of the contact parameters, such as the mean contact pressure, the contact area and the contact load as a function of the contact interference are modeled in the elastic, elastic-plastic and fully plastic contact regime. Verification of the model is made using the experimental results and is compared with published theoretical models. Compared to the prediction of the other contact models, very good agreement between the present model and the experimental results are found.*

*Key words: contact mechanics, elastic-plastic, spherical asperity.*

### Introduction

Contact deformation occurs when two engineering surfaces are pressed together. Depending on the scale considered, this contact deformation can be categorized as; macro-contact and micro-contact. Most surfaces are rough on micro-scale. High points or micro-protrusions, usually called asperities, exist on most engineering solid surfaces, see Figure 1. In non-lubricated or boundary lubrication systems, when such surfaces are loaded against each other, the actual contact takes place at these asperities. Contact will initially occur at a limited amount of asperities and the number of asperities in contact becomes larger as the normal load increases. Depending upon the load carried by the asperities and its mechanical properties, the asperities may deform elastic, elastic-plastic or fully plastic [1].

The deformation states of the surface asperities are very important in studying friction, wear, lubrication, electrical contact resistance, etc. Plastic deformation changes the surface topography. Understanding the relationship between local contact properties and surface topography can lead to the specification of optimized surface topography and manufacturing processes with respect to the desired functional properties of the surface. Research has been performed in order to model the deformation behaviour of the bodies in contact [2-15]. This was pioneered by Greenwood and Williamson [2]. In their model a nominal flat surface is assumed to be composed with spherical asperities of the same radius and the height of the asperities is represented by a well-defined statistical distribution function (i.e. Gaussian). The contact analysis is based on the Hertz theory [3] where the asperities deform elastically. This elastic asperity-based model has been extended to the contact of rough curved surfaces [4], the contact of two nominally flat rough surfaces with misaligned asperities [5], the contact of rough surfaces considering the distribution of the radii of the asperities [6] and elliptic paraboloidal surfaces [7]. However, the aforementioned models are devoted to the elastic contact situation.

Abbot and Firestone [8] introduced the basic plastic contact model which is known as the profilometric model or surface micro-geometry model. In this model the deformation of a rough surface against a smooth rigid flat is assumed to be equivalent to the truncation of the undeformed rough surface at its intersection with the flat so that the contact area is simply the geometrical intersection of the original profile. The mean contact pressure is equal to the flow pressure or the indentation hardness of the softer body. Based on the experimental results, Pullen and Williamson [9] proposed a volume conservation model for the fully plastic contact of a rough surface. Kucharski *et al.* [10] confirmed this model by the finite element analysis.

In order to bridge the two extreme models, elastic and fully plastic, Chang *et al.* (CEB model) [11] developed an elastic-plastic contact model based on volume conservation of the plastically deforming asperities. In the CEB model there is no transition regime from the elastic

to the fully plastic contact regime while Johnson [12] showed, based on the analysis of the indentation of a sphere on a plane, that there is a long transition regime from the point of initial yielding to the fully plastic state. Therefore, Zhao *et al.* (ZMC model) [13] proposed a new elastic-plastic contact model which includes this transition by mathematical smoothing expressions to incorporate the elastic and fully plastic contact parameters. Kogut and Etsion (KE model) [14] performed a detailed finite element analysis on the elastic-plastic contact of a sphere and a rigid flat. The empirical coefficients for the dimensionless relations for contact load, contact area and mean contact pressure as a function of contact interference have been provided. However, the analysis is limited up to the onset of the fully plastic state. A similar work has been done recently by Jackson and Green (JG model) [15].

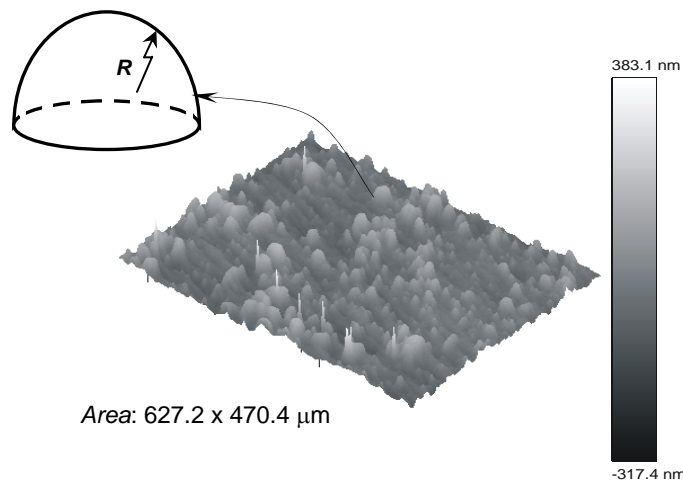


Figure 1. Engineering surface and its asperities.

This paper presents a new elastic-plastic contact model of a sphere against a hard flat. Its main features are the modeling of the transition from elastic-plastic to fully plastic contact regime and the modeling of the mean contact pressure in the fully plastic contact regime. The results show that such parameters play an important role in the analysis of the contact behavior. Studies of this field have been done extensively by the author by changing the contact parameters [16-20].

### Elastic Contact

When contact interference  $\omega$  is sufficiently small the asperity deforms elastically. For the elastic contact of a flat against a sphere of radius  $R$ , according to the Hertz theory [3], the contact area  $A_e$ , the contact load  $P_e$  and the mean contact pressure  $p_e$  of the asperity can be expressed in term of  $\omega$  as:

$$A_e = \pi R \omega \quad (1)$$

$$P_e = \frac{4E}{3} R^{0.5} \omega^{1.5} \quad (2)$$

$$p_e = \frac{4E}{3\pi} \left( \frac{\omega}{R} \right)^{0.5} \quad (3)$$

It was shown by the work of Tabor [21] that initial yield occurs when the maximum Hertz contact pressure reaches  $p_m = 0.6H$ , or, the average contact pressure  $p_e = 0.4H$  where  $H$  is the

hardness of the softer material in contact. For a more general representation this relation can be written as:

$$p_m = K_v H \quad (4)$$

According to Chang *et al.* [22], based on the von Mises failure criteria, the value of  $K_v$  in Equation (4) is related to the Poisson's ratio  $\nu$  as:

$$K_v = 0.454 + 0.41\nu \quad (5)$$

Substituting Equation (4) into Equation (3) yields the critical interference  $\omega_1$  (elastic to elastic-plastic):

$$\omega_1 = \left( \frac{\pi K_v H}{2E} \right)^2 R \quad (6)$$

### Plastic Contact

When  $\omega$  is increased to another critical value  $\omega_2$  at which the mean contact pressure  $p$  of the asperity reach its maximum, fully plastic deformation occurs. Most researchers have reported that this maximum value equals to its hardness  $H$ . However, it was shown recently by Jamari and Schipper [23] using a more accurate measurement that in the fully plastic contact regime the mean contact pressure reach its maximum and remain constant at a value lower than its hardness, or:

$$p_p = c_h H \quad (7)$$

where  $c_h$  is the hardness coefficient for the fully plastic contact regime.

The contact area  $A_p$  was found by [23] the same as was reported by [8], and is equal to the geometrical intersection of the flat with the original undeformed profile of the asperity:

$$A_p = 2\pi R \omega \quad (8)$$

The contact load  $P_p$  of the asperity is equal to the contact area multiplied by the mean contact pressure. Or

$$P_p = 2\pi R \omega c_h H \quad (9)$$

The solid expression for the onset of fully plastic interference  $\omega_2$  (elastic-plastic to plastic) is not known, therefore it will be estimated. A simple analysis, similar to [13], is done based on the contact load. At  $\omega = \omega_2$ , the contact load is equal to Equation (9). At the same time, the contact load had it been elastic as would be equal to Equation (2). Therefore, the following inequality can be established:

$$2\pi R \omega_2 c_h H < \frac{4E}{3} R^{0.5} \omega_2^{1.5} \quad (10)$$

Or

$$\omega_2 > \left( \frac{3\pi c_h H}{2E} \right)^2 R = \frac{9c_h^2}{K_v^2} \left( \frac{\pi K_v H}{2E} \right)^2 R \quad (11)$$

Substituting Equation (6) into Equation (11) yields,

$$\omega_2 > 9 \left( \frac{c_h}{K_v} \right)^2 \omega_1 \quad (12)$$

With  $c_h = 0.75$  and  $K_v = 0.6$ , one obtains

$$\omega_2 > 14\omega_1 \quad (13)$$

The minimum value of  $\omega_2$  may also be further estimated using experimental results. The fully plastic regime of a half-space indented by a rigid sphere according to Francis [24] starts at  $A/A_c = 113.2$  and according to Johnson [12] full plasticity starts at  $Ea/YR \approx 40$  or  $P/P_c \approx 360$  where  $A_c$  and  $P_c$  is the critical contact area and the critical contact load, respectively, at the initial yield point and  $Y$  is the yield stress. Based on the experimental results of Chaudhri *et al.* [25] for the contact problem of a deformable sphere and a rigid flat, the fully plastic contact regime (as indicated by a constant mean contact pressure) starts at  $A/A_c \approx 60$  for phosphor-bronze and 100 for brass if  $A/A_c$  is calculated according to the JG model. Or in general:

$$\frac{A}{A_c} = c_A \quad (14)$$

Substituting Equations (1) and (8) into Equation (14) and rearranging results into:

$$\frac{\omega_2}{\omega_1} = \frac{c_A}{2} \quad (15)$$

### Elastic-Plastic Contact

In the present study the approach as used in the ZMC model will be utilized to analyze the elastic-plastic contact problem of a sphere against a hard flat. The ZMC model employed the statistical analysis of spherical indentations of Francis [24] where the mean contact pressure in the elastic-plastic contact regime may be represented by a logarithmic function. By using the constant  $c_h$  for the fully plastic contact regime and following the approach of ZMC, the mean contact pressure  $p_{ep}$ , the contact area  $A_{ep}$  and the contact load  $P_{ep}$  in the elastic-plastic contact regime are:

$$p_{ep} = c_h H - H \left( c_h - \frac{2}{3} K_v \right) \frac{\ln \omega_2 - \ln \omega}{\ln \omega_2 - \ln \omega_1} \quad (16)$$

$$A_{ep} = \pi R \omega \left[ 1 - 2 \left( \frac{\omega - \omega_1}{\omega_2 - \omega_1} \right)^3 + 3 \left( \frac{\omega - \omega_1}{\omega_2 - \omega_1} \right)^2 \right] \quad (17)$$

$$P_{ep} = A_{ep} \left[ c_h H - H \left( c_h - \frac{2}{3} K_v \right) \frac{\ln \omega_2 - \ln \omega}{\ln \omega_2 - \ln \omega_1} \right] \quad (18)$$

### Results and Discussions

To illustrate the developed model, the experimental elastic-plastic contact data of Chaudhri [25] will be used for validation. The results are also plotted along with the theoretical predictions of the CEB model, the ZMC model, the KE model and the JG model. Chaudhri [25] performed experiments on the elastic-plastic contact of phosphor-bronze ( $H = 2.72$  GPa,  $E = 115$  GPa and  $\nu = 0.35$ ) and brass ( $H = 1.8$  GPa,  $E = 115$  GPa and  $\nu = 0.35$ ) spheres of 3.17 mm diameter in contact with a sapphire ( $H = 190$  GPa,  $E = 430$  GPa and  $\nu = 0.26$ ) plate. In his experiments, the contact area was measured directly in the elastic and the elastic-plastic contact

regime but for the fully plastic contact regime the contact area was measured indirectly or after the load is removed. In the elastic to elastic-plastic contact experiments, the sphere was compressed between a load cell and a transparent sapphire plate so that the contact area can be measured directly by a microscope.

Figure 2 and 3 show the non-dimensional mean contact pressure  $p/(c_h H)$  as a function of the non-dimensional contact area  $A/A_c$  for phosphor-bronze and brass material, respectively. It can be seen from the figures that the proposed elastic-plastic contact model fit very well with the experimental results from the elastic to the fully plastic contact regime. In these cases, the coefficient of hardness  $c_h = 0.805$  and the contact area constant  $c_A = 40$  for phosphor-bronze and  $c_h = 0.967$  and  $c_A = 90$  for brass. In Figure 2, the theoretical predictions of the ZMC model, the KE model and the JG model predict a higher mean contact pressure for the contact area higher than the critical contact area in the onset of elastic-plastic regime, while the JG model predicts a lower mean contact pressure. The ZMC and KE model predict an increasing mean contact pressure as the contact area increases until the non-dimensional contact area value  $A/A_c = 108$  and  $A/A_c = 220$ . Beyond these values the mean contact pressure will stay constant at the hardness indentation value. Instead of the indentation hardness parameter the JG model used the yield stress parameter. There is no yield stress data available, therefore, in the present analysis the yield stress was assumed to be  $H/2.8$  [21].

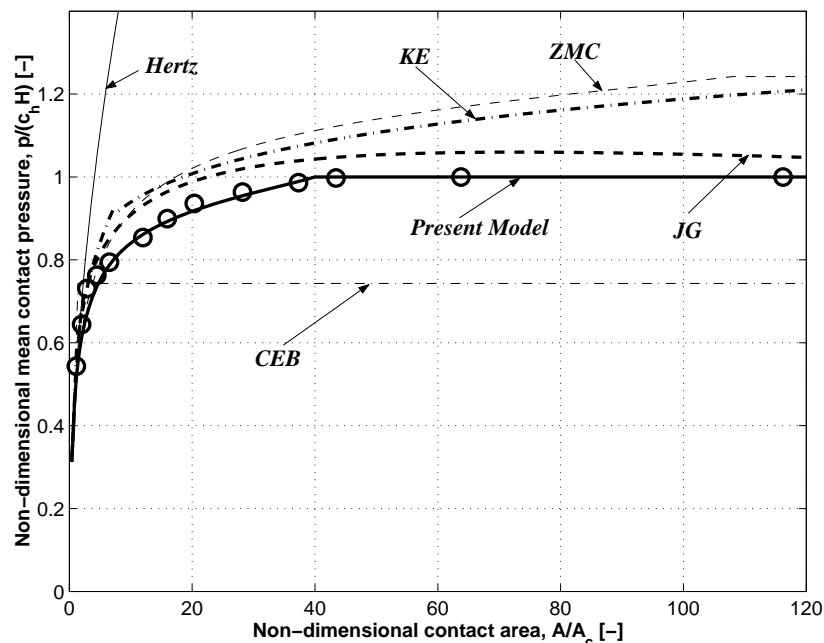


Fig. 2. Non-dimensional mean contact pressure vs non-dimensional contact area.  
 ○ phosphor-bronze experimental data [25].

The JG model predicts the mean contact pressure as a function of the contact area differently. The mean contact pressure increases as the contact area increases, however, for a certain value of the contact area the mean pressure reaches a maximum value and then start to decrease as the contact area increases. As can be seen in Figure 2 and 3 the maximum contact pressure of the JG model occurs at a value of  $A/A_c \approx 70$  for phosphor-bronze and  $A/A_c \approx 110$  for brass. For a relatively high value of the contact area the mean contact pressure can reach a value even lower than the CEB model. The CEB model predicts the mean contact pressure in the elastic-plastic and fully plastic contact regimes lower than the other models because in this model there is no transition regime from the elastic to fully plastic and the mean contact pressure is assumed  $p_p = K\nu H$  in the fully plastic regime.

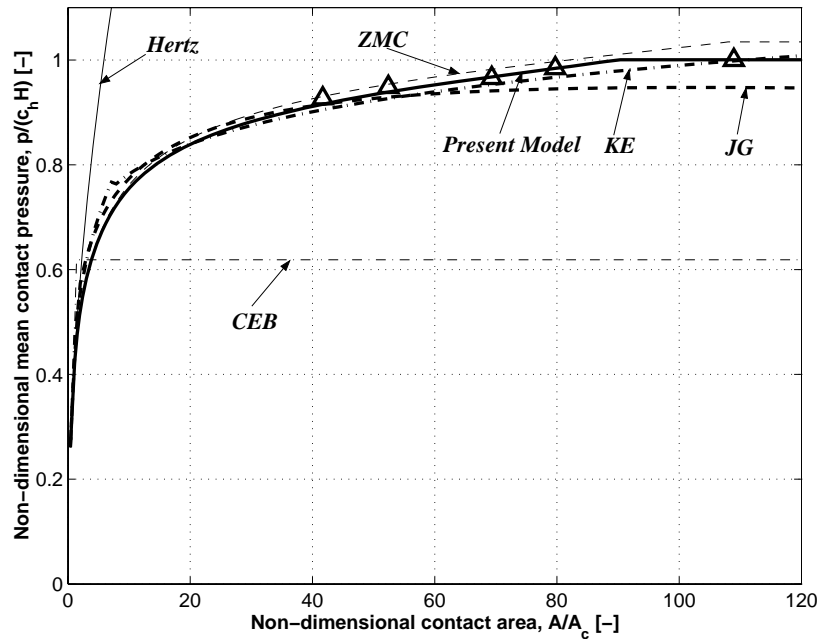


Fig. 3. Non-dimensional mean contact pressure vs non-dimensional contact area.  
 $\Delta$  brass experimental data [25].

Figure 4 and 5 present the results of the non-dimensional contact area  $A/A_c$  as a function of the non-dimensional normal load  $P/P_c$  for phosphor-bronze and brass, respectively. As can be seen the new developed elastic-plastic contact model predicts the contact behaviour best among the others. The CEB model overestimates the contact area as a function of the contact load because the mean contact pressure predicted by the CEB model is lower than the actual one. For the phosphor-bronze the ZMC, KE and JG models underestimates the contact area as the load increases for all the experimental data but for the brass these models almost coincide for a relatively low load. However, for the brass case, as the load increases the JG model start to deviate and overestimates the contact area. The ZMC and KE models predict the contact area as the load increases rather well.

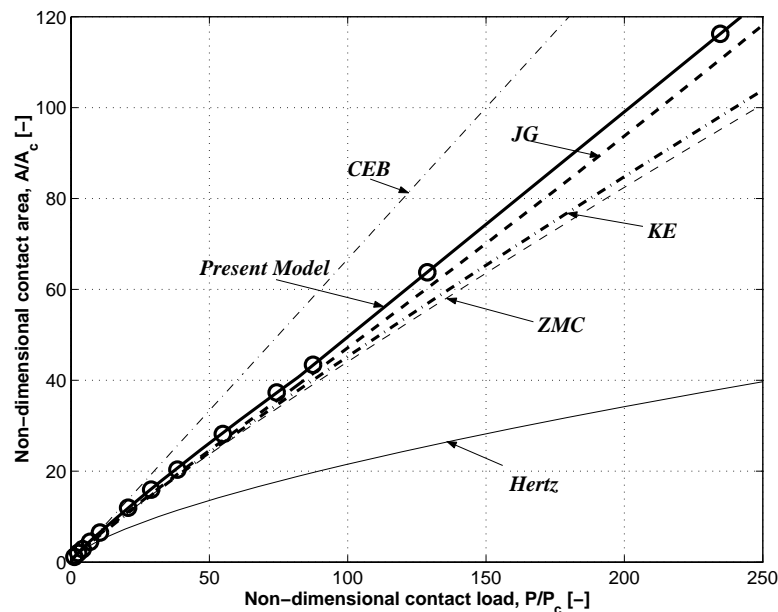


Fig. 4. Non-dimensional contact area vs non-dimensional contact load.  
 $\circ$  phosphor-bronze experimental data [25].

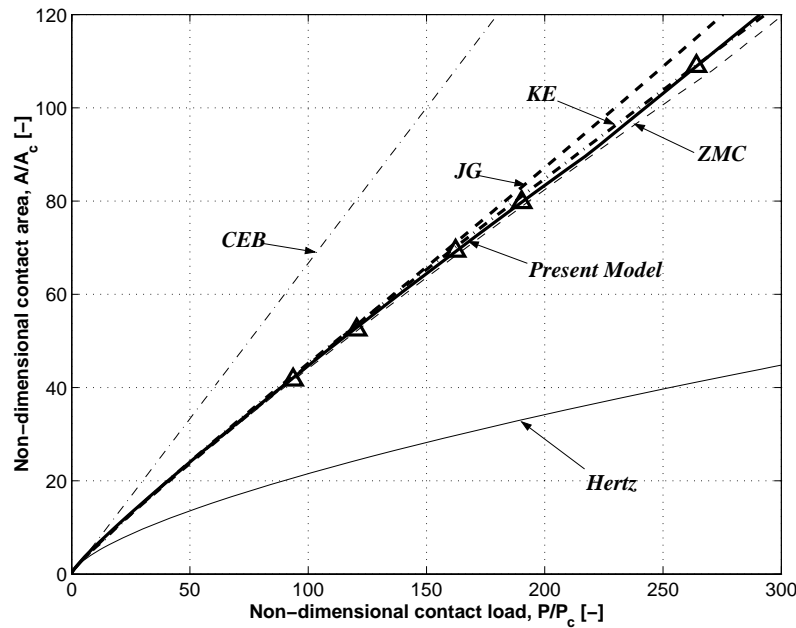


Fig. 5. Non-dimensional contact area vs non-dimensional contact load.  
 $\Delta$  brass experimental data [25].

### Conclusions

A theoretical model for the normal contact of elastic-plastic of a sphere against a hard flat has been presented. Formulae describing the contact parameters have been developed in order to predict the contact behaviour. The developed model was compared with published experimental and theoretical data in terms of the mean contact pressure, the contact area and the contact load.

It was found that the developed model predicts the contact behaviour best among other models. In the fully plastic contact regime the mean contact pressure is observed to be lower than the indentation hardness as often reported. The transition from the elastic to the elastic-plastic state is almost the same for all the proposed models. However, in this study, the transition from the elastic-plastic to the fully plastic is found depending on the material properties. Substantial differences were shown in the comparison between the present model with the available proposed models.

### References

1. Bhushan, B., 1996, "Contact Mechanics of Rough Surfaces in Tribology: Single Asperity Contact," *ASME Applied Mechanics Review* **49**, pp. 275-298.
2. Greenwood, J.A. and Williamson, J.B.P., 1966, "Contact of Nominally Flat Surfaces," *Proc. R. Soc. London* **A295** pp.300-319.
3. Timoshenko, S. and Godier, J.N., 1951, *Theory of Elasticity*, McGraw-Hill, New York.
4. Greenwood, J.A. and Tripp, J.H., 1967, "The Elastic Contact of Rough Spheres," *ASME Journal of Applied Mechanics* **34** pp. 153-159.
5. Greenwood, J.A. and Tripp, J.H., 1970-71, "The Contact of Two Nominally Flat Rough Surfaces," *Proc. Instn. Mech. Engrs.* **185** pp. 625-633.
6. Hisakado, T., 1974, "Effect of Surface Roughness on Contact between Solid Surfaces," *Wear* **28** pp. 217-234.
7. Bush, A.W., Gibson, R.D. and Thomas, T.R., 1975, "The Elastic Contact of Rough Surface," *Wear* **35** pp. 87-111.
8. Abbott, E.J. and Firestone, F.A., 1933, "Specifying Surface Quality — A Method Based on Accurate Measurement and Comparison," *Mech. Engr.* **55** p. 569.
9. Pullen, J. and Williamson, J.B.P., 1972, "On the Plastic Contact of Rough Surfaces," *Proc. R. Soc. London* **A327** pp. 159-173.
10. Kucharski, S., Klimczak, T., Polijaniuk, A. and Kaczmarek, J., 1994, "Finite Element Model for the Contact of Rough Surfaces," *Wear* **177** pp. 1-13.

11. Chang, W.R., Etsion, I. and Bogy, D.B., 1987, "An Elastic-Plastic Model for the Contact of Rough Surfaces," *ASME Journal of Tribology* **109** pp. 257-263.
12. Johnson, K.L., 1985, *Contact Mechanics*, Cambridge University Press, Cambridge.
13. Zhao, Y., Maietta, D.M. and Chang, L., 2000, "An Asperity Microcontact Model Incorporating the Transition from Elastic Deformation to Fully Plastic Flow," *ASME Journal of Tribology* **122** pp. 86-93.
14. Kogut, L. and Etsion, I., 2002, "Elastic-Plastic Contact Analysis of a Sphere and a Rigid Flat," *ASME Journal of Applied Mechanics* **69** pp. 657-662.
15. Jackson, R.L. and Green, I., 2005, "A Finite Element Study of Elasto-Plastic Hemispherical Contact against a Rigid Flat," *ASME Journal of Tribology* **127** pp. 343-354.
16. Jamari, J. and Schipper, D.J., 2006, "An Elastic-Plastic Contact Model of Ellipsoid bodies," *Tribology Letters* **21** pp. 262-271.
17. Jamari, J. and Schipper, D.J., 2006, "Deformation Due to Contact Between a Rough Surface and a Smooth Ball," *Wear*, article in press.
18. Jamari, J. and Schipper, D.J., 2006, "Plastic Deformation and Contact Area of an Elastic-Plastic Contact of Ellipsoid Bodies after Unloading," *Tribology International*, accepted for publication.
19. Jamari, J. and Schipper, D.J., 2006, "Criterion for Surface Deformation," *Tribotest*, accepted for publication.
20. Jamari, J. and Schipper, D.J., 2006, "Plastic Deterministic Contact of Rough Surfaces," *ASME Journal of Tribology*, accepted for publication.
21. Tabor, D., 1951, *The Hardness of Metals*, Oxford university press.
22. Chang, W.R., Etsion, I. and Bogy, D.B., 1988, "Static Friction Coefficient Model for Metallic Rough Surfaces," *ASME Journal of Tribology* **110** pp. 57-63.
23. Jamari, J. and Schipper, D.J., 2006, "Experimental Investigation of Fully Plastic Contact of a Sphere against a Hard Flat," *ASME Journal of Tribology* **128** pp. 230-235.
24. Francis, H.A., 1976, "Phenomenological Analysis of Plastic Spherical Indentation," *ASME Journal of Engineering Material Technology* **98** pp. 272-281.
25. Chaudhri, M.M., Hutchings, I.M. and Makin, P.L., 1984, "Plastic Compression of Spheres," *Philosophical Magazine* **A49** pp. 493-503.